Acta Crystallographica Section B
Structural Science
ISSN 0108-7681

Revision of pyrrhotite structures within a common superspace model

Zunbeltz Izaola,[a]* Santiago González,[a] Luis Elcoro,[a] J. M. Perez-Mato,[a] Gotzon Madariaga[a] and Alberto García[b]

[a]Dpto de Física de la Materia Condensada, Facultad de Ciencia y Tecnología, Universidad del País Vasco, Apdo 644, Bilbao 48080, Spain, and [b]Institut de Ciencia de Materials de Barcelona, CSIC Campus de la UAB, E-08193 Bellaterra, Spain

Correspondence e-mail: wmbizazz@ehu.es

Received 10 February 2007
Accepted 30 July 2007

The structure of pyrrhotite ($Fe_{1-x}S$ with $0.05 \leq x \leq 0.125$) has been reinvestigated in the framework of the superspace formalism. A common model with a centrosymmetric superspace group is proposed for the whole family. The atomic domains in the internal space representing the Fe atoms are parametrized as crenel functions that fulfil the closeness condition. The proposed model explains the x-dependent space groups observed and the basic features of the structures reported up to now. Our model yields for any x value a well defined ordered distribution of Fe vacancies in contrast to some of the structural models proposed in the literature. A new $(3+1)$-dimensional refinement of $Fe_{0.91}S$ using the deposited dataset [Yamamoto & Nakazawa (1982). *Acta Cryst.* A**38**, 79–86] has been performed as a benchmark of the model. The consistency of the proposed superspace symmetry and its validity for other compositions has been further checked by means of *ab initio* calculations of both atomic forces and equilibrium atomic positions in non-relaxed and relaxed structures, respectively.

1. Introduction

Over the last few years, an increasing number of families of compounds with variable composition have been analysed or reanalysed within a unifying framework provided by the superspace formalism (Evain *et al.*, 1998; Perez-Mato *et al.*, 1999; Elcoro *et al.*, 2000, 2001; Boullay *et al.*, 2002, 2003; Lind & Lidin, 2003; Michiue *et al.*, 2005, 2006). All these families have several common characteristics. Their members can be interpreted as the result of atomic occupational modulations over a common parent structure, which is usually a member of the family for a special or limiting composition. For each composition, the three-dimensional structure can be viewed as the regular stacking of a small number of different layers, their sequence (and therefore the stacking period and the size of the unit cell) being determined by the composition. In most cases, while the building blocks in the parent structure are *complete* layers, the building units for the rest of the members of the family also include layers that result from an ordered removal of atoms in the complete layers (*vacancy layers*), or from an ordered substitution of some atoms by atoms of a different element (*defect layers*). Usually, there are several different (but equivalent by translation) *vacancy* or *defect* layers. The *vacancy* or *defect* layers stack among the *complete* ones forming ordered sequences that depend on composition. Usually, within a stacking sequence there are (periodic or aperiodic) blocks of consecutive layers which are globally shifted with respect to the neighbouring blocks. Due to this property, these compound families are sometimes called *crystallographic shear structures* (Andersson & Wadsley,

© 2007 International Union of Crystallography
Printed in Singapore – all rights reserved

1966). In the superspace description, the atomic voids in the vacancy layers or the atomic substitution in the defect layers are introduced using so-called crenel functions (Petříček *et al.*, 1995), *i.e.* step-like (zero/one) occupational atomic modulations yielding atomic domains (ADs) in internal space analogous to those present in quasicrystals (Steurer, 2004). An essential feature of the superspace description of these families is the fulfilment by some ADs of the so-called *closeness* condition. According to this property, the lower limit of the projection onto the internal space of an AD coincides with the upper limit of the projection of another AD which is equivalent by a superspace translation. This yields, in general, real-space configurations where the atomic motifs or vacancies represented by these ADs are distributed within the layers as regularly as possible, producing so-called *uniform* sequences (Elcoro *et al.*, 2001). In general, the closeness condition forces a specific linear relationship of the composition (associated with the size of these ADs) with the modulation wavevector (modulation parameter), and therefore with the size of the superstructure unit cell. These are the basic features that allow a global description in the superspace of a series of layered compounds. Furthermore, it is an empirical observation that the different space-group symmetries realised for different compositions can be explained by a unique common superspace group, while the atomic modulation functions (AMF) describing the displacive distortions are very similar for all members of a given series, and thus weakly dependent on the length of the layer sequence.

The pyrrhotites, *i.e.* binary compounds of the type $Fe_{1-x}S$, can be described as layered compounds where sulfur layers intercalate with *complete* and *vacancy* Fe layers, forming stacking sequences that depend on x and can yield very long periods (*i.e.* large unit cells) or even incommensurate configurations (Bertaut, 1953; Tokonami *et al.*, 1972; Koto *et al.*, 1975; Yamamoto & Nakazawa, 1982; Powell *et al.*, 2004). One can therefore infer that these compounds might also be described by a single superspace model. In 1982 the pyrrhotite $Fe_{0.91}S$ was in fact the object of one of the first quantitative structural analyses carried out using the superspace formalism and was described as an incommensurate system (Yamamoto & Nakazawa, 1982). Already in this work it was suggested that the same approach could be appropriate for the description of other members with different composition, including commensurate ones. However, at this early stage in the application of the superspace formalism, only continuous occupational modulations with truncated short Fourier series could be used. This implied that the structural models could not include discontinuous atomic domains and therefore could not describe configurations with fully ordered vacancies. In this situation no relation between the modulation wavevector and composition was presumed or detected, and furthermore the superspace group that was proposed and used for the specific composition investigated was not compatible with the three-dimensional space groups of other commensurate pyrrhotites such as Fe_7S_8 and $Fe_{11}S_{12}$. Nowadays, the refinement of (3 + 1)-dimensional superspace models with occupational crenel functions describing discontinuous ADs along the internal subspace is feasible with the program *JANA*2000 (Petříček *et al.*, 2000), and much empirical knowledge about the use of the superspace formalism in ordered systems with flexible composition has been gathered.

In this context, we present here a revision of the existing experimental evidence on the pyrrhotites. Considering an idealized layer model for several compositions, and following the general rules observed in other families, we propose a common superspace structural model with ADs fulfilling the closeness condition. A linear relationship between composition and the modulation parameter is obtained. The superspace symmetry underlying the whole family is found to be different from that used by Yamamoto & Nakazawa (1982), being a non-trivial supergroup of it. The model has been crosschecked successfully with the published experimental data. As a way of visualizing and confirming the superspace symmetry that we propose, we also present the results of *ab initio* calculations analysed in a novel form. The forces acting on the atoms when located in idealized layered configurations for several compositions have been calculated and embedded in superspace. In addition, in some cases the structures have been relaxed and the equilibrium configuration has been calculated and analysed in superspace. In both cases, the compliance with the symmetry of the proposed superspace group was confirmed.

This paper is organized as follows: the next section gives a summary of previous approaches to the structure description of these compounds, paying special attention to the incommensurate case analysed by Yamamoto & Nakazawa (1982). Next, the new superspace model (based on discontinuous ADs) and its symmetry is introduced. Subsequently, a comparison with the available experimental evidence is given, including a new refinement of the dataset of Yamamoto & Nakazawa (1982) for $Fe_{0.91}S$ based on this model. Finally, the results of the *ab initio* calculations are presented.

2. Pyrrhotite structures

$Fe_{1-x}S$ is commonly found in nature in the $0.05 < x < 0.125$ composition range. The structures can be interpreted as metal-deficient NiAs-type structures, with the Fe vacancies distributed rather uniformly. The NiAs-type compound [which can be considered the ideal (*parent*) structure for the pyrrhotite family, with $x = 0$] has an hexagonal structure with $a_H = b_H \simeq 3.5$, $c_H \simeq 5.7$ Å, $\alpha = \beta = 90$, $\gamma = 120^\circ$, space group $P6_3/mmc$ and two independent atoms in the unit cell: Fe at the origin and S at $\left(\frac{1}{3}, \frac{2}{3}, \frac{1}{4}\right)$. The S atoms form a hexagonal close-packed structure and the Fe atoms locate in the octahedral interstices between successive S layers. For rational values of the composition parameter in the pyrrhotite family, the resulting structures are pseudo-orthorhombic with similar a and b cell parameters, and a c unit length which depends on composition. The three known structures of pyrrhotite have monoclinic (pseudo-orthorhombic) symmetry, with similar $a = 2a_H$ and $b = 2a_H + 4b_H$ unit-cell vectors. The c parameter depends on the compositions: $c = 4c_H$ for $x = 1/8$ (Fe_7S_8, known as $4C$), $c = 6c_H$ for $x = 1/12$ ($Fe_{11}S_{12}$, known as $6C$;

Bertaut, 1953; Tokonami *et al.*, 1972; Koto *et al.*, 1975; Powell *et al.*, 2004) and the incommensurate $Fe_{0.91}S$ compound (Yamamoto & Nakazawa, 1982) with $x \simeq 0.09$. In this setting the symmetries for commensurate 4*C* and 6*C* compounds have been reported as $F2/d11$ and $F1d1$, respectively. A fourth trigonal polymorph of Fe_7S_8 has also been observed (Fleet, 1971; Nakano *et al.*, 1979; Keller-Besrest *et al.*, 1983), but it is outside the present study.

Fig. 1 shows the projection of the parent structure onto the (x, y) plane also showing the ideal orthorhombic cell corresponding to the actual lattice of the 4*C* and 6*C* compounds. Omitting the S layers (which are always fully occupied), the commensurate cation-deficient pyrrhotite structures can be described in a first approximation as the layer stacking of fully occupied Fe layers (in the following denoted as F) and six-atom layers of four kinds, A, B, C and D. The labels of these four different layers indicate the positions of the two vacancies (A, B, C or D positions in Fig. 1). The Fe_7S_8 structure (Bertaut, 1953; Tokonami *et al.*, 1972; Powell *et al.*, 2004) is characterized by the layer stacking sequence FAFBFCFD. In this way the vacancies form a double helix whose axis is parallel to the **c** direction. The compound $Fe_{11}S_{12}$ was analysed in Koto *et al.* (1975) and a model with some Fe disorder was proposed, but not quantitatively refined. The vacancies were 'divided' into two equivalent sites of consecutive layers with occupancy 1/2 for each position, leading to the stacking sequence $FP_AP_AFP_BP_BFP_CP_CFP_DP_D$, where P_i represents a one-half occupied *i*-position layer. Within fully ordered configurations the closest layer arrangement would be obviously described by the stacking sequence FFAFFBFFCFFD. In this sequence, the vacancies also form a double helix, but with a different step than in the case of $x = 1/8$.

In Yamamoto & Nakazawa (1982) a third compound with the composition $x \simeq 0.09$ was investigated. The structure was considered as incommensurately modulated with a modulation wavevector of the form $\mathbf{q} = \gamma\mathbf{c}^*_H = 0.1805\mathbf{c}^*_H$ ($\simeq 2/11\mathbf{c}^*_H$) and superspace group $Pna2_1(\frac{1}{2}\frac{1}{2}\gamma)qq0$ (equivalent to No. 33.3

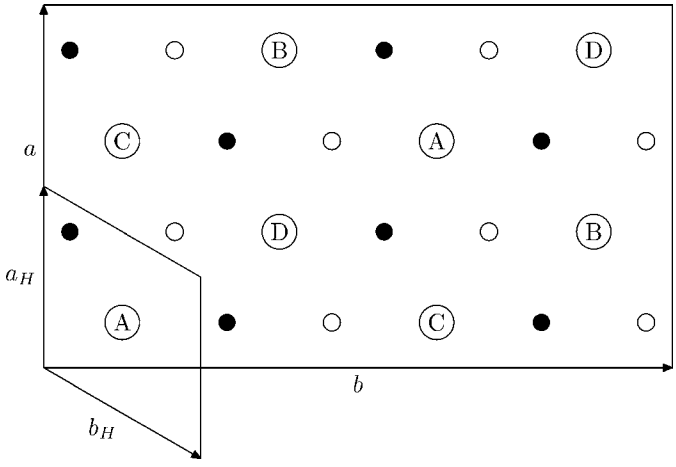

Figure 1
Projection of the parent structure of pyrrhotites onto the (x, y) plane. Large circles represent Fe atoms with the same z coordinate, labelled with four letters A, B, C and D. Small black dots and small open circles represent S atoms in a plane above and below the Fe layer, respectively.

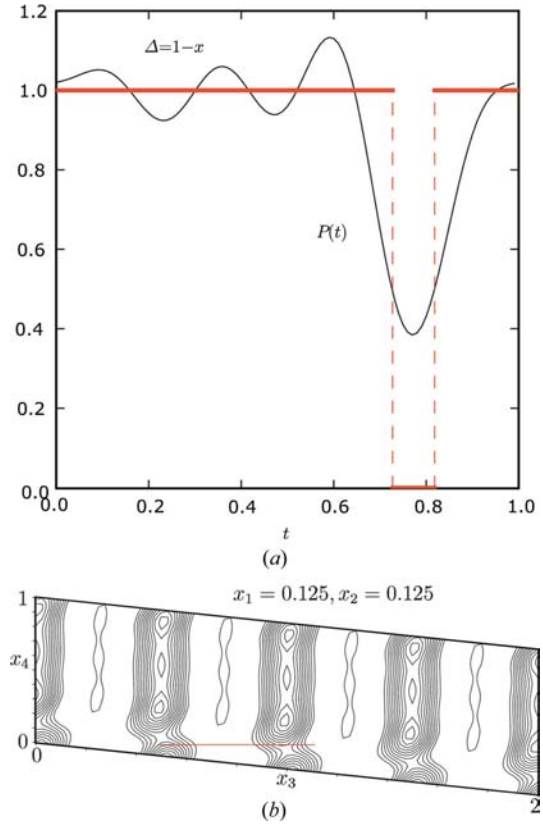

Figure 2
(*a*) Occupation function for the independent Fe atom in the model of Yamamoto & Nakazawa (1982) (solid continuous line), and crenel function representing the same atom in the model discussed in §3 (horizontal discontinuous line). (*b*) Electron density in the $(1/8, 1/8, x_3, x_4)$ superspace plane. The horizontal line indicates that the closeness condition is fulfilled.

in the *International Tables for Crystallography* (Janssen *et al.*, 1992).[1] The structure was modelled with just two independent ADs in the superspace unit cell, representing the S and Fe atoms of the parent structure described in Fig. 1. According to this model, the AD of sulfur is continuous and fully occupied along the internal space. On the contrary, the AD associated with the Fe atom is described by a continuous function, $P(x_4)$, representing the occupation probability depending on the internal coordinate x_4. The refined occupation function of the Fe atom showed a narrow valley along x_4 with a low occupation probability, while the rest of the x_4 interval was close to full occupation (Fig. 2*a*, equivalent to Fig. 2*d* in Yamamoto & Nakazawa, 1982). The displacive AMFs for S and Fe atoms have small amplitudes, indicating that all atoms are very close to the ideal layer positions (see Figs. 2*a*, *b* and *c* in Yamamoto & Nakazawa, 1982). Therefore, the resulting structure could also be viewed as the regular and alternate stacking of S and Fe layers. The location in superspace of the occupation holes in the function $P(x_4)$ of the Fe atom means that some of the Fe layers can be considered fully occupied, with eight atoms, and other Fe layers have six fully occupied positions and two with

[1] We use here a different setting from that in Yamamoto & Nakazawa (1982). The **a** and **b** axes have been interchanged to accommodate the setting used in the analysis of the other pyrrhotites.

Table 1
Structural parameters in the superspace description of the pyrrhotite $Fe_{1-x}S$: centres of the independent ADs $(x_1^0, x_2^0, x_3^0, x_4^0)$ without modulation, width of the crenel functions Δ, point symmetry of the ADs and symmetry of the $[u_1(x_4), u_2(x_4), u_3(x_4)]$ modulation functions with respect to their centres, x_4^0.

Atom	x_1^0	x_2^0	x_3^0	x_4^0	Δ	Point symmetry	Displacive modulation
Fe	1/8	1/8	0	5/8	$1-x$	211	(even,odd,odd)
S	1/8	−1/24	3/4	1/8	1	121	(odd,even,odd)

low occupation probabilities, reproducing a pattern of Fe layers similar to that of the 4*C* commensurate structure. The continuous description of the Fe occupation probability however introduces some disorder in the positions of the vacancies, with some sites having partial occupation.

3. Unique superspace model for the $Fe_{1-x}S$ compounds

The occupational modulation function $P(x_4)$ for the Fe atoms obtained by Yamamoto & Nakazawa (1982) using a Fourier series parametrization is reminiscent of a crenel function of width $1-x$ (~ 0.91; see Fig. 2*a*). The fact that the reported experimental modulus of the modulation wavevector fulfils the relation $\gamma = 2x$ within experimental accuracy, with x being the iron deficiency, is a hint that points to a model with crenel functions. Such a type of correlation is expected when crenel functions are subject to the closeness condition (see §1). Furthermore, the Fourier map of Fig. 2(*b*), equivalent to Fig. 6(*a*) in Yamamoto & Nakazawa (1982), indicates that the closeness condition would be fulfilled by the inferred crenels. Taking into account the information above and the fact that there are four different (but equivalent by translation) vacancy Fe layers, and two different S layers, the simplest superspace model which gives the correct sequence for the 4*C* ($x = 1/8$) and 6*C* ($x = 1/12$) phases is represented in Fig. 3. For this construction we have followed the same general principles explained in Elcoro *et al.* (2003). The thin and thick bars represent the superposition of eight different ADs located at the mentioned (x, y) coordinates for S and Fe atoms, respectively. As the ADs representing Fe atoms are crenel functions, the vertical bars are divided into segments of width $1/4 - x$, labelled F and coloured in black, where eight ADs superpose resulting in full occupation (layers with eight atoms), and segments of width x coloured in grey where only six ADs superpose, corresponding to six-atom layers, and labelled A, B, C and D according to the (x, y) coordinates of the missing ADs that define the layer vacancies (see Fig. 1). The relation $\gamma = 2x$ between the modulation parameter γ and the composition parameter is assumed. This relation forces the closeness condition between the x_4 segments corresponding to vacancies/layers of the same type (see the dotted line in Fig. 3). The atomic structural parameters of this model are summarized in Table 1, including the symmetry of the displacive AMFs associated with the independent atoms. The superspace group of this ideal construction is $Pbnn\left(\frac{1}{2}\frac{1}{2}\gamma\right)qq0$ (No. 52.7 in *International Tables of Crystallography*). As in Yamamoto & Nakazawa (1982), to avoid the rational components in the modulation wavevector, we have considered a non-standard centered unit cell, which implies the doubling of the *a* and *b* unit-cell parameters with respect to those used in a standard primitive unit cell. The symmetry operations are given in Table 2, including centring translations.

Table 2
Centring translations and rotational symmetry elements of the $Pbnn\left(\frac{1}{2}\frac{1}{2}\gamma\right)qq0$ superspace group, but with a different centring, with $\mathbf{q} = (0, 0, \gamma)$ as the modulation vector (see the text).

$\{E\|0,0,0,0\}$	$\{E\|1/2,0,0,1/2\}$	$\{E\|0,1/2,0,1/2\}$	$\{E\|1/2,1/2,0,0\}$
$\{E\|0,0,0,0\}$	$\{m_x\|0,1/4,0,1/4\}$	$\{m_y\|1/4,0,1/2,1/4\}$	$\{2_z\|1/4,1/4,1/2,0\}$
$\{I\|0,0,0,0\}$	$\{2_x\|0,1/4,0,1/4\}$	$\{2_y\|1/4,0,1/2,1/4\}$	$\{m_z\|1/4,1/4,1/2,0\}$

At this point, it is important to compare the superspace group used in Yamamoto & Nakazawa (1982) and that proposed here. The essential difference is the addition of an inversion centre. Apart from the interchange of the x and y axes to have a common setting for the commensurate and incommensurate structures, the origin here is that shown in Fig. 1, in contrast to that used by Yamamoto & Nakazawa (1982), which is located on the Fe atom [$(x, y) = (1/8, 1/8)$ position in Fig. 1]. Therefore, in the setting used by Yamamoto & Nakazawa (1982), the inversion centre of the postulated superspace group here would be located at the non-trivial point $(1/8, 1/8, 0)$, and therefore may have been overlooked there. In fact, the addition of the inversion centre introduces the following reflection condition: $h + k = 4n$ for $(h, k, 0, 0)$ reflections (due to the operation $\{m_z|1/4, 1/4, 1/2, 0\}$) and this condition is indeed fulfilled by the dataset deposited by Yamamoto & Nakazawa (1982).

The assumption of a higher symmetry has another important consequence. In the structural model of Yamamoto &

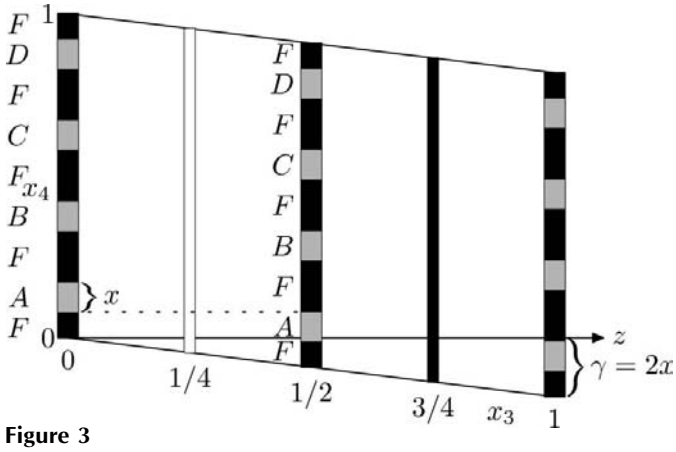

Figure 3
Ideal superspace model for the pyrrhotite compound family. White (black) thin bars at $x_3 = 1/4$ (3/4) represent S layers with (x, y) atomic coordinates given by the black dots and small open circles, respectively, in Fig. 1. Thick bars at $x_3 = 0$ and 1/2 represent Fe layers. Black bars denoted by the F letter are complete eight-atom layers, and A, B, C and D bars represent the six-atom layers with two vacancies located at the corresponding A, B, C and D locations of Fig. 1. The dotted line shows the closeness condition.

Table 3
Resulting three-dimensional space groups for the superspace group of Table 2 with commensurate $\gamma = r/s$ and different values of the t internal coordinate.

Space groups in bold are *non-problematic* cases (see the text).

s = odd	$\boldsymbol{t = 0 (\mathrm{mod}\ 1/4s)}$ $\boldsymbol{C112_1/d}$	$t = 1/8 (\mathrm{mod}\ 1/4s)$ $C222_1$	$\boldsymbol{t}$ = **arbitrary** $\boldsymbol{C112_1}$
$s = 4N$	$\boldsymbol{t = 0 (\mathrm{mod}\ 1/2s)}$ $\boldsymbol{F2/d11}$	$t = 1/4s (\mathrm{mod}\ 1/2s)$ $Fd2d$	$\boldsymbol{t}$ = **arbitrary** $\boldsymbol{Fd11}$
$s = 4N + 2$	$t = 0 (\mathrm{mod}\ 1/2s)$ $F12/d1$	$\boldsymbol{t = 1/4s (\mathrm{mod}\ 1/2s)}$ $\boldsymbol{F2dd}$	$\boldsymbol{t}$ = **arbitrary** $\boldsymbol{F1d1}$

Table 4
R values for main and satellite reflections of the refined model for $x = 0.0903$ with data from Yamamoto & Nakazawa (1982).

For comparison, the values obtained with the model proposed in this reference are included. The latter values vary in some cases significantly from those reported in that publication.

		Present model		Yamamoto & Nakazawa (1982)		
No. of parameters	Indep. ref./obs. ($I>2\sigma$)	45 R(obs)	R(all)	64 R(obs)	R(all)	R_{int}
Total	588/391	11.52	14.19	10.38	15.95	51.81
Main ref. ($m = 0$)	71/45	6.23	6.49	5.76	6.57	50.96
Satellites $m = 1$	134/120	14.05	16.51	12.73	19.83	52.84
Satellites $m = 2$	126/75	7.16	9.48	10.00	16.58	50.41
Satellites $m = 3$	135/109	27.31	35.78	21.99	35.04	54.72
Satellites $m = 4$	122/44	60.22	88.13	35.48	82.46	51.75
GoF(obs)/GoF(all)		5.65	4.81			
$\rho_{\mathrm{max}}/\rho_{\mathrm{min}}$		122.71	−5.81			

Nakazawa (1982) the independent atomic domains occupy general Wyckoff positions. This means that the modulations have no symmetry restrictions. In a model with discontinuous ADs this would mean that the centres of the ADs are not fixed by symmetry. As a consequence, the closeness condition is not forced by the relation $\gamma = 2x$ and may only be introduced as an additional *ad-hoc* restriction. However, if the superspace group of Table 2 is assumed, the point symmetries of the Fe and S independent domains are 211 and 121, respectively. Thus, the centre of the AD representing the Fe atom is fixed in the (x_3, x_4) projection (see Fig. 3), and the closeness condition is fulfilled once the modulation parameter γ is given the value $2x$. It is noticeable that, in the model of Yamamoto & Nakazawa (1982), despite not being fixed by the superspace group, the positions of the low-occupancy Fe regions fulfil the closeness condition. This fact reinforces the idea that the superspace group of Table 2 is the correct symmetry of this system.

Table 3 shows the possible three-dimensional space groups resulting from the proposed superspace group, for commensurate values of the modulation parameter. The space group of the resulting three-dimensional structure depends both on the type of fraction for the modulation parameter γ and on the global initial phase of the modulation, *i.e.* the t value of the three-dimensional section in the superspace construction. When step-like (crenel) atomic domains are used, some t values are problematic, namely those for which the three-dimensional section crosses the limits of some atomic domains (the points at which the occupation probability changes from 0 to 1). For these sections, the assumed three-dimensional structure becomes ambiguous and a full consistency with the assumed superspace symmetry would require the splitting of the occupational probability, hence modifying the initial structural model. These problematic t values typically correspond to high-symmetry sections due to the closeness condition relating the modulation parameter with the width of the crenels. In Table 3 the t values not having this problem are indicated in bold. These are the three-dimensional symmetries which are fully compatible with the superspace model and are to be expected for commensurate values of x. This table is consistent with the space group reported for the $4C$ ($\gamma = \frac{1}{4}$) phase (Bertaut, 1953; Tokonami *et al.*, 1972; Powell *et al.*, 2004), which corresponds to the case $s = 4N$ and $t = 0$. The symmetry $F1d1$ proposed for the $6C$ ($\gamma = 1/6$) phase in Koto *et al.* (1975) is also in accordance with the prediction for such a type of modulation parameter, but for an arbitrary t value. This is quite atypical, as special t sections corresponding to higher symmetries are usually realised in commensurate structures. This makes us suspect that also in this case some symmetry may have been overlooked. We infer from Table 3 that the three-dimensional space group would instead be $F2dd$ if the iron vacancies are fully ordered or $F12/d1$ in the case of some iron disorder.

4. New refinement of $Fe_{0.91}S$

The validity of the proposed superspace model has been tested by performing a new refinement of the $x \simeq 0.09$ compound, $Fe_{0.91}S$, using the dataset provided by Yamamoto & Nakazawa (1982). According to the reported value of the modulation parameter $\gamma = 0.1805$, we have assumed a composition given by $x = \gamma/2 = 0.0903$ and therefore the width of the iron crenel function was set to $1 - x = 0.90975$. The refinement was performed using the software package *JANA*2000 (Petříček *et al.*, 2000). Starting from the ideal structure defined in Table 1 and outlined in Fig. 3, only average coordinates and thermal coefficients[2] were refined in the first steps of the refinement with a resulting residual factor of 40%. Afterwards, successive Fourier terms in the expansion series for the displacive AMFs have been introduced for both the Fe and S ADs. As the width of the crenel functions representing Fe atoms is close to 1, there are no correlation problems between the first harmonics used in the Fourier expansion series, and no orthogonalized functions have been used. Thermal coefficients for the Fe AD have been modulated. The refinement is stable and converges rapidly. This process led to a global $R = 0.14$ ($R = 0.11$ for observed reflections), with 45 refinable parameters with significant values. In the final model, the x, y and z coordinates of the Fe and S atoms are described by four

[2] We use the term *thermal coefficient* instead of the standard *atomic displacement parameter*, because in this context they could be confusing.

Table 5
Refined parameters for $_{Fe0.91}S$.

Cell parameters are a = 6.892, b = 11.952 and c = 5.744 Å. The fractional atomic average coordinate, atomic positional and DWF modulation coefficients are modeled using Fourier expansion for the modulation. Modulation functions for a parameter λ of an atom ν defined in a restricted interval are given by the following: $U^{\nu}_{\lambda}(x_4) = \sum_{n=0}^{k} A^{\nu}_{\lambda,n} \sin 2\pi n x_4 + \sum_{n=0}^{k} B^{\nu}_{\lambda,n} \cos 2\pi n x_4$, where k is the number of modulation functions used for each atomic domain. Parameters with no standard deviation (in parenthesis) are fixed by symmetry. (*a*) Parameters defining the position and width for the atomic domains in the four-dimensional structure. (*b*) Parameters of the displacive modulations. (*c*) Parameters of the thermal coefficients. We have used the term *thermal coefficient* rather than the standard *atomic displacement parameter* because in this context it could be confusing.

(*a*)

Atom	x_1	x_2	x_3	x_4	Δ
Fe	0.1265 (5)	0.125	0	5/8	0.90975
S	0.125	−0.0426 (2)	0.75	–	1

(*b*)

$A^{Fe}_{x,1} = 0.0130$ (5)	$A^{Fe}_{y,1} = -0.0042$ (2)	$A^{Fe}_{z,1} = -0.0062$ (5)	$B^{Fe}_{x,1} = 0.0130$	$B^{Fe}_{y,1} = 0.0042$	$B^{Fe}_{z,1} = 0.0062$
$A^{Fe}_{x,2} = 0.0019$ (8)	$A^{Fe}_{y,2} = 0$	$A^{Fe}_{z,2} = 0$	$B^{Fe}_{x,2} = 0$	$B^{Fe}_{y,2} = -0.0100$ (2)	$B^{Fe}_{z,2} = 0.0094$ (6)
$A^{Fe}_{x,3} = -0.0044$ (5)	$A^{Fe}_{y,3} = 0.0016$ (2)	$A^{Fe}_{z,3} = 0.0050$ (5)	$B^{Fe}_{x,3} = 0.0044$	$B^{Fe}_{y,3} = 0.0016$	$B^{Fe}_{z,3} = 0.0050$
$A^{Fe}_{x,4} = 0$		$A^{Fe}_{z,4} = 0.0020$ (6)	$B^{Fe}_{x,4} = -0.0021$ (9)		$B^{Fe}_{z,4} = 0$
	$A^{S}_{y,1} = -0.0005$ (2)	$A^{S}_{z,1} = -0.0106$ (8)		$B^{S}_{y,1} = -0.0006$	$B^{S}_{z,1} = 0.0106$
	$A^{S}_{y,2} = -0.0008$ (3)	$A^{S}_{z,2} = 0$		$B^{S}_{y,2} = 0$	$B^{S}_{z,2} = -0.0142$ (9)
		$A^{S}_{z,3} = 0.0037$ (7)			$B^{S}_{z,3} = 0.0037$
		$A^{S}_{z,4} = -0.0032$ (9)			$B^{S}_{z,4} = 0$

(*c*)

$U^{Fe,0}_{U11,0} = 0.010$ (2)	$U^{Fe}_{U22,0} = 0.016$ (1)	$U^{Fe}_{U33,0} = 0.010$ (2)	$U^{Fe}_{U12,0} = 0$	$U^{Fe}_{u13,0} = 0$	$U^{Fe}_{u23,0} = 0.0002$ (10)
$U^{S}_{u_{iso}} = 0.0072$ (9)					
$A^{Fe}_{U11,1} = -0.006$ (2)	$A^{Fe}_{U22,1} = -0.004$ (1)	$A^{Fe}_{U33,1} = -0.006$ (4)	$B^{Fe}_{U11,1} = -0.006$	$B^{Fe}_{U22,1} = -0.004$	$B^{Fe}_{U33,1} = -0.006$
$A^{Fe}_{U12,1} = 0.019$ (9)	$A^{Fe}_{U13,1} = 0.0006$ (11)	$A^{Fe}_{U23,1} = 0.0007$ (11)	$B^{Fe}_{U12,1} = -0.019$	$B^{Fe}_{U13,1} = -0.0006$	$B^{Fe}_{U23,1} = 0.0007$
$A^{Fe}_{U11,2} = -0.016$ (4)	$A^{Fe}_{U22,2} = -0.003$ (2)	$A^{Fe}_{U33,2} = -0.005$ (4)	$B^{Fe}_{U11,2} = 0$	$B^{Fe}_{U22,2} = 0$	$B^{Fe}_{U33,2} = 0$
$A^{Fe}_{U12,2} = 0$	$A^{Fe}_{U13,2} = 0$	$A^{Fe}_{U23,2} = 0.005$ (1)	$B^{Fe}_{U12,2} = -0.008$ (1)	$B^{Fe}_{U13,2} = -0.008$ (2)	$B^{Fe}_{U23,2} = 0$
$A^{Fe}_{U11,3} = -0.011$ (2)	$A^{Fe}_{U22,3} = -0.007$ (2)	$A^{Fe}_{U33,3} = -0.014$ (3)	$B^{Fe}_{U11,3} = 0.011$	$B^{Fe}_{U22,3} = 0.007$	$B^{Fe}_{U33,3} = 0.014$
$A^{Fe}_{U12,3} = 0.0028$ (9)	$A^{Fe}_{U13,3} = -0.0006$ (11)		$B^{Fe}_{U12,3} = 0.0028$	$B^{Fe}_{U13,3} = -0.0006$	
$A^{Fe}_{U11,4} = 0$		$A^{Fe}_{U33,4} = 0$	$B^{Fe}_{U11,4} = 0.016$ (3)		$B^{Fe}_{U33,4} = 0.022$ (3)
$A^{Fe}_{U12,4} = 0.002$ (1)	$A^{Fe}_{U13,4} = -0.003$ (2)		$B^{Fe}_{U12,4} = 0$	$B^{Fe}_{U13,4} = 0$	

harmonics. For S atoms an isotropic thermal coefficient has been used and for the Fe AD an anisotropic thermal coefficient, modulated with four harmonics, was needed. The final R values for main and satellite reflections are given in Table 4 and the resulting refined structural parameters are listed in Table 5. Table 4 also includes the R values of the model presented in Yamamoto & Nakazawa (1982). The two refinements under the two models have similar quality. Some partial indices are somewhat worse in the present model, especially that for fourth-order observed satellites, but the number of refined parameters is significantly smaller (45 against 64). If the number of parameters is increased up to a similar value, fully comparable R values are obtained. However, even under this significant decrease of the structural parameters, first- and second-order satellites are better fitted and as a consequence the total R value for all reflections is also significantly lower.

The projection of the resulting independent ADs onto the (x_3, x_4) plane is outlined in Fig. 4. As can be seen in the figure, the atomic displacements of the atoms with respect to the ideal positions are small, with very smooth AMFs. The displacements along the x and y directions with respect to the ideal positions are also small. The reduction of the number of parameters with respect to the model of Yamamoto & Nakazawa (1982) is due to the higher symmetry used and the better adapted description of the occupation modulation of the Fe atom by means of a crenel function. It means that the distribution of vacancies can also be considered ordered in this more complex composition, as happens in the 4C phase. In terms of layers, the aperiodic stacking sequence corresponding

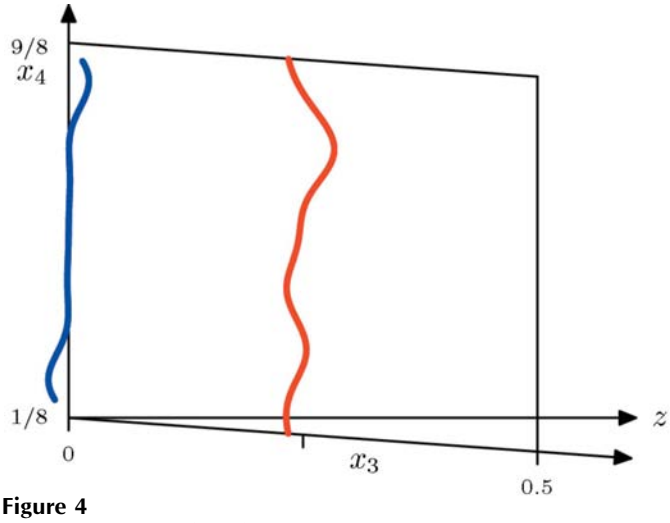

Figure 4
Projection onto the (x_3, x_4) plane of two independent atomic domains of $Fe_{0.90975}S$, Fe in $x_3 = 0$ and S in $x_3 = 1/4$ according to the refined model listed in Table 5.

to this composition, close to $x = 1/11$, is dominated by sets of 22 layers following the sequence $(AFFBFFCFFDF)^2$ (or equivalent ones) separated by 'faults' giving a final aperiodic but deterministic sequence.

5. Superspace symmetry in *ab initio* calculations

The superspace model proposed above includes two essential features that modify the approach of Yamamoto & Nakazawa (1982). On one hand, the use of crenel functions with the closeness condition implies full ordering of the iron vacancies and a general relation between the composition and the number of layers in the unit cell for a commensurate case, or a linear relationship between the modulation wavevector and the composition in an incommensurate case. On the other hand, an inversion centre is added to the superspace symmetry previously considered. This allows us to understand the observed three-dimensional space groups as particular cases of the underlying $(3 + 1)$-dimensional superspace symmetry. We have shown above that the available experimental evidence is consistent with this model and its symmetry. However, some doubts can still be raised. Concerning the assumption of vacancy ordering, as mentioned above, the 6*C* compound has been claimed to have some disorder with partial iron occupancies (Koto *et al.*, 1975). We cannot rule out the possibility that indeed some systematic disorder may happen for some compositions, but it is clear that the detailed experimental evidence for the other two compounds can be consistently described with fully ordered configurations following the general scheme given by our superspace model. Even the 6*C* disordered configuration proposed in Koto *et al.* (1975) complies with the symmetry properties of this model and its main features become evident if the proposed partial occupied iron vacancies are substituted by fully occupied and vacant iron sites. Furthermore, a fully ordered model would explain the 12-layer period of the compound.

A more delicate point is the symmetry that is actually realised in these compounds. Establishing the presence or absence of an inversion centre by means of X-ray diffraction data is always difficult. The actual existence or not of an inversion centre in the superspace symmetry underlying these structures is of special importance, since the absence of the inversion centre would mean that these systems, for some compositions, would be polar through a small displacive distortion with respect to a non-polar configuration with symmetry given by either $C112_1/d$ or $F2/d11$. As these systems have ferromagnetic or antiferromagnetic phases, this would imply the possibility of a multiferroic character, with coupling of ferroelectric and (*anti*)ferromagnetic properties (Fiebig, 2005). Note that even for the centrosymmetric superspace symmetry, for some compositions the three-dimensional structures are also polar (see Table 3), but in these cases no ferroelectric properties are expected. For these compositions the ordered iron vacancy configuration is already polar, and this polarity would not be in principle switchable, as it would require a drastic vacancy reordering.

In order to further investigate the validity of the proposed superspace group we have performed *ab initio* calculations to analyze the fully relaxed atomic positions for the 4*C* and 6*C* structures, and to obtain atomic forces in the ideal vacancy configuration for a longer-period $x = 1/11$ structure. The results have been embedded and analysed in superspace. The calculations have been carried out with *SIESTA* (Soler *et al.*, 2002), a density-functional code which is able to handle large unit cells owing to its efficient strictly localized basis sets. Fe and S pseudopotentials with core corrections (Louie *et al.*, 1982) were generated in the ground-state configurations, with a cutoff radius of 0.894 Å for S and $r_s = r_d = 1.15$ and $r_p = r_f = 1.26$ Å for Fe. We have used the revised Perdew–Burke–Enzerhof exchange-correlation functional (Hammer *et al.*, 1999), an optimized (Junquera *et al.*, 2001) double-ζ plus polarization basis set, with first-ζ cutoffs for *s*, *p* and *d* orbitals of 2.35, 2.30 and 3.02 Å for Fe, and 2.63, 3.21 and 2.56 Å for S, and a 250 Ry cutoff for the real-space mesh. The forces on the atoms follow from the Hellmann–Feynman theorem, as implemented in the code.

We studied first the case $x = 1/8$. Starting from an ideal layer structure following the layer stacking sequence predicted by the superspace model above and with the lattice parameters fixed to the experimental values, the atomic positions were relaxed with no rotational symmetry restriction and the equilibrium configuration was determined. The points in Figs.

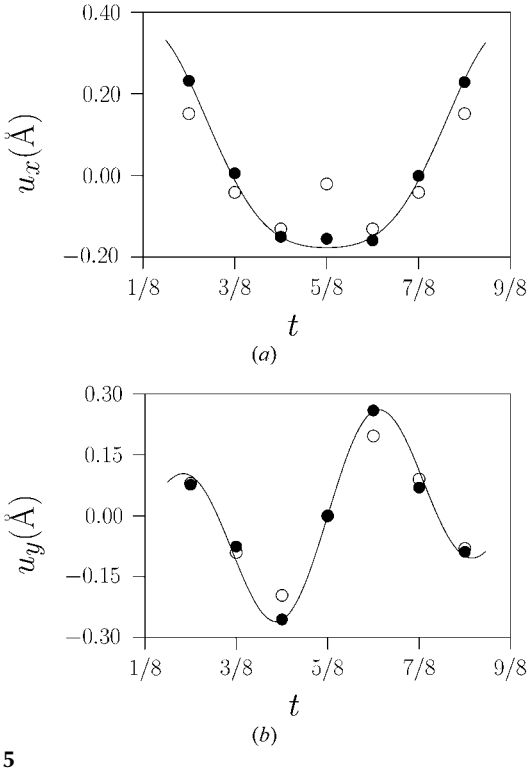

Figure 5
Case $x = 1/8$. Comparison of experimental (Powell *et al.*, 2004) (empty circles) and calculated (solid circles) displacements of the Fe atoms along the *x* (*a*) and *y* (*b*) direction. Atomic displacements with respect to the ideal layer position are represented within a single independent AD in superspace using the assumed superspace symmetry. The continuous line depicts a fit of the calculated points using a symmetry adapted truncated Fourier series.

5(*a*) and (*b*) are graphs of representative examples of the results. The displacements along the *x* and *y* directions of the Fe atoms with respect to the ideal structure are represented as discrete points along the internal coordinate of superspace. The calculated displacements have been embedded into a single AD using the assumed superspace symmetry. The smoothness of the AMF that can be extrapolated from these discrete points confirms the adequacy of the postulated superspace symmetry. The inversion centre in the superspace group forces the AMF components along the *x* and *y* directions to be symmetric and antisymmetric, respectively, with respect to the centre of the occupation domain (see Table 1). The deviations of the calculated atomic displacements from this expected symmetry are negligible. Furthermore, the displacements agree reasonably well with those derived from experiment (Powell *et al.*, 2004), as shown in Fig. 5. This result is especially significant considering that our prediction for the magnetic order of the calculated ground state is ferromagnetic, in contrast with the experimental observation of an antiferromagnetic phase (Powell *et al.*, 2004). This points to a very weak magneto-structural coupling in these compounds and allows us to take with confidence these calculations for other compositions, despite the failure to reproduce the magnetic state.

A similar study was carried out for the composition $x = 1/12$ (phase 6*C*). Fig. 6 depicts results analogous to those in Fig. 5 for this case. The superspace embedding of the Fe displacements from their ideal layer positions in the calculated equilibrium configuration are compared with that corresponding to the case where $x = 1/8$ and with the experimental AD of Fe in the incommensurate case where $x = 0.0903$, according to the refinement discussed above (Table 5). Again, only very small deviations of the atomic displacements from the expected symmetry or antisymmetry of the AMFs with respect to the AD centre are obtained. A similarity of the underlying AMFs for the commensurate cases with the one of the incommensurate case can be clearly seen. A broad common pattern can be observed in the three cases, but one cannot speak about invariance of the displacive modulations with composition, as differences are quite significant. The (composition dependent) fluctuations of the AMFs along the *z* direction around the centre of the AD are especially noticeable. The general pattern of the AMF of iron along the *z* direction can be easily interpreted. The displacements tend to be larger at the extreme of the ADs where the Fe atoms have a neighbouring Fe vacancy at the subsequent Fe layer, either above or below. These atoms therefore suffer a strong displacement towards the vacancy in order to locally compensate the charge. The antisymmetry of the function is forced by this behaviour. Regions of the AD which are closer to the centre represent those Fe atoms which are the farthest from Fe vacancies at the same (*x*, *y*) position in other layers. Therefore, they are expected to move less. The Fe atom represented by the centre of the AD has nearest-neighbouring Fe vacancies at the same distance along the vertical both above and below, in accordance with its null displacement. However, if only neighbouring vacancies along the vertical are considered one cannot explain the fluctuating pattern of the AMF. This must be due to the competing effect of vacancies away from the vertical in neighbouring layers. Indeed, the AD of Fe can be divided into segments according to the type of local coordination they imply for the corresponding Fe atomic sites considering the neighbouring layers below and above along the *z* axis. One can then see that the AD regions where the *z* displacement changes sign (with respect to the direction where the nearest vertical vacancy is) correspond to x_4 segments where a vacancy layer with non-vertical vacancies is closer in the opposite direction.

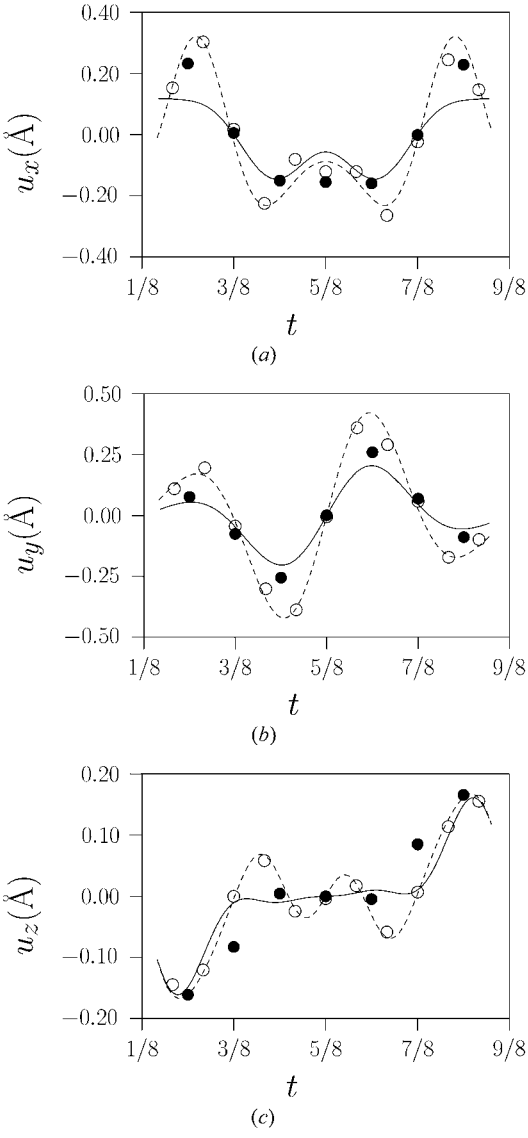

Figure 6
Comparison of calculated displacements of Fe atoms along the *x* (*a*), *y* (*b*) and *z* (*c*) direction for the compositions $x = 1/8$, $x = 1/12$ and the refined AMFs for the incommensurate case $x = 0.0903$ (Table 5). Atomic displacements have been embedded in superspace within a single independent AD using the assumed superspace group. The continuous line represents the AMF of the incommensurate case close to $x = 1/11$. Solid and empty circles correspond to $x = 1/8$ and 1/12, respectively. The dashed line represent a fit of the calculated points for the $x = 1/12$ case.

An energy relaxation for a commensurate case corresponding to a much more dense set of discrete points in the superspace embedding than those discussed above would require a much larger computational cost. For instance, for $x = 1/11$, which would be very close to the incommensurate composition of the compound refined above, the number of independent atoms is 42, in comparison to 12 in the case of $x = 1/12$. However, in this case we can have at least an impression of the superspace symmetry underlying the structure relaxation if we embed in superspace the forces that the atoms exhibit at the idealized perfect layer configuration, without trying the much more costly process of determining the relaxed structure that cancels these forces. In the same way as the atomic positions, the calculated atomic forces can be associated with a single independent AD for each atom type if, after the superspace embedding, the assumed superspace group is used to produce symmetry equivalent forces within a single AD. Fig. 7 shows a scheme of the result obtained for the case $x = 1/11$ for the z component of the forces, which are in general much larger than the forces on the (x, y) plane. From the 40 (44) forces on the Fe (S) atoms, that are represented in the figure, 20 (22) are symmetry independent according to the three-dimensional space group $C1121/d$ that is fulfilled by the structure (see Table 3). In fact, when the three-dimensional structure is embedded into superspace, only 11 S and 10 Fe atoms are realised within a single AD of each atomic type. The grouping together of the 40 Fe and 44 S values is obtained assuming the superspace group described in Table 2. The symmetry elements relate the different ADs and can be used to transport all discrete values realised in differents ADs into a single independent one. Forces depicted as consecutive along x_4 are not symmetry-related in the three-dimensional structure and correspond to atoms quite far apart in the three-dimensional structure, but as the figure shows, they are clearly correlated. Hence, not only do the atomic positions vary smoothly along the internal space in a single AD, also other physical properties (in this case the forces) behave as continuous functions along the internal space. This demonstrates the efficiency of the superspace model that has been postulated. The systematic fluctuation of the forces along the ADs reflects the division of the ADs into segments according to the type of vacancy coordination of the atomic sites that they are representing, as discussed above. In all cases, the forces on the Fe atoms are directed towards the nearest vacancy. The strongest forces are suffered by Fe atoms located just below/above a vacancy along the **c** direction. In fact, it can be seen that the AMF describing the iron z displacements of the experimental structure represented in Fig. 6(*c*) follow a pattern very similar to that of the forces depicted in Fig. 7.

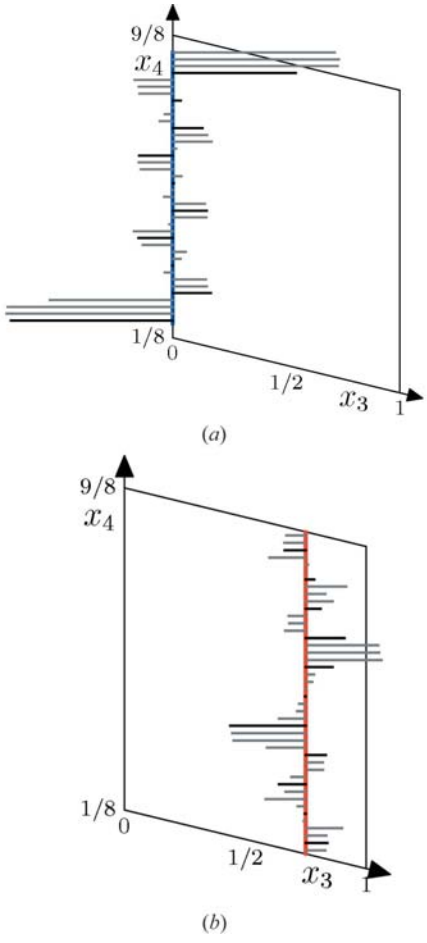

Figure 7
Calculated atomic forces along the **c** direction in $Fe_{10/11}S$ for its ideal perfect-layer configuration, with displacive AMFs set to zero. Forces are represented embedded in superspace within a single AD for Fe (*a*) and S (*b*). Black horizontal bars represent forces at atomic sites which correspond to the depicted AD, while gray bars correspond to other ADs that have been 'transported' by means of the superspace group operations. The largest force is of the order of 0.7 eV Å^{-1}.

6. Conclusions

The results presented here show that the pyrrhotite structures can be described with a unique superspace model and a common superspace symmetry. The main feature of the model is the assumption of crenel (step-like) functions to represent the Fe atoms in superspace. As a consequence, the resulting three-dimensional structures are ordered. The superspace symmetry of the common model corrects that which had been proposed previously for a specific compound. The atomic correlations described by the proposed superspace model have been checked by *ab initio* calculations of the forces acting on the atoms for an idealized configuration with perfect layers. The embedding of the calculated atomic forces in the superspace shows that they can also be described by continuous modulation functions and they are interrelated according to the proposed superspace group.

This work has been supported by UPV/EHU (Project 00063.310-13564) and Ministerio de Ciencia y Tecnología (MAT2005-05216). S. González is grateful for the financial support obtained from the Spanish Government (MEC) by an FPU grant. The SGI/IZO-SGIker of the UPV/EHU (supported by the Ministerio de Educación, Fondo Social Europeo, Ministerio de Ciencia y Tecnologíay Gobierno

Vasco) is gratefully acknowledged for the generous allocation of computational resources.

References

Andersson, S. & Wadsley, A. D. (1966). *Nature*, **211**, 581.
Bertaut, E. F. (1953). *Acta Cryst.* **6**, 557–561.
Boullay, Ph., Teneze, N., Troilliard, G., Mercurio, D. & Perez-Mato, J. M. (2003). *J. Solid State Chem.* **174**, 209–220.
Boullay, Ph., Trolliard, G., Mercurio, D., Perez-Mato, J. M. & Elcoro, L. (2002). *J. Solid State Chem.* **164**, 261–271.
Elcoro, L., Perez-Mato, J. M., Darriet, J. & El Abed, A. (2003). *Acta Cryst.* B**59**, 217–233.
Elcoro, L., Perez-Mato, J. M. & Withers, R. (2000). *Z. Kristallogr.* **215**, 727–739.
Elcoro, L., Perez-Mato, J. M. & Withers, R. L. (2001). *Acta Cryst.* B**57**, 471–484.
Evain, M., Boucher, F., Gourdon, O., Petricek, V., Dusek, M. & Bezdicka, P. (1998). *Chem. Mater.* **10**, 3068–3076.
Fiebig, M. (2005). *J. Phys. D Appl. Phys.* **38**, R123–R152.
Fleet, M. E. (1971). *Acta Cryst.* B**27**, 1864–1867.
Hammer, B., Hansen, L. B. & Norskov, J. K. (1999). *Phys. Rev. B*, **59**, 7413–7421.
Janssen, T., Janner, A., Looijenga-Vos, A. & de Wolf, P. M. (1992). *International Tables for Crystallography*, edited by A. J. C. Wilson, Vol. C, p. 797. Dordrecht, The Netherlands: Kluwer Academic Publishers.
Junquera, J., Paz, O., Sánchez-Portal, D. & Artacho, E. (2001). *Phys. Rev. B*, **64**, 235111.
Keller-Besrest, F., Collin, G. & Comès, R. (1983). *Acta Cryst.* B**39**, 296–303.
Koto, K., Morimoto, N. & Gyobu, A. (1975). *Acta Cryst.* B**31**, 2759–2764.
Lind, H. & Lidin, S. (2003). *Solid State Sci.* **5**, 47–57.
Louie, S. G., Froyen, S. & Cohen, M. L. (1982). *Phys. Rev. B*, **26**, 1738–1742.
Michiue, Y., Yamamoto, A., Onoda, M., Sato, A., Akashi, T., Yamane, H. & Goto, T. (2005). *Acta Cryst.* B**61**, 145–153.
Michiue, Y., Yamamoto, A. & Tanaka, M. (2006). *Acta Cryst.* B**62**, 737–744.
Nakano, A., Tokonami, M. & Morimoto, N. (1979). *Acta Cryst.* B**35**, 722–724.
Perez-Mato, J. M., Zakhour-Nakhl, M., Weill, F. & Darriet, J. (1999). *J. Mater. Chem.* **9**, 2795–2808.
Petříček, V., Dusek, M. & Palatinus, L. (2000). *JANA*2000. Institute of Physics, Praha, Czech Republic.
Petříček, V., van der Lee, A. & Evain, M. (1995). *Acta Cryst.* A**51**, 529–535.
Powell, A. V., Vaqueiro, P., Knight, K. S., Chapon, L. C. & Sanchez, R. D. (2004). *Phys. Rev. B*, **70**, 014415.
Soler, J. M., Artacho, E., Gale, J. D., García, A., Junquera, J., Ordejón, P. & Sánchez-Portal, D. (2002). *J. Phys. Condens. Matter*, **14**, 2745–2779.
Steurer, W. (2004). *Z. Kristallogr.* **219**, 391–446.
Tokonami, M., Nishiguchi, N. & Morimoto, N. (1972). *Am. Mineral.* **57**, 1066–1080.
Yamamoto, A. & Nakazawa, H. (1982). *Acta Cryst.* A**38**, 79–86.